Inorganic Chemistry

Communication

pubs.acs.org/IC

Gallium Analogue of Soluble Prussian Blue $KGa[Fe(CN)_6]\cdot nH_2O$: Synthesis, Characterization, and Potential Biomedical Applications

Murthi S. Kandanapitiye,[†] Benjamin Valley,[†] Liu D. Yang,[†] Allyson M. Fry,[‡] Patrick M. Woodward,*[,‡] and Songping D. Huang*[,†]

[†]Department of Chemistry and Biochemistry, Kent State University, Kent, Ohio 44240, United States

[‡]Department of Chemistry and Biochemistry, The Ohio State University, Columbus, Ohio 43210, United States

Supporting Information

ABSTRACT: The gallium analogue of the soluble Prussian blue with the formula $KGa[Fe(CN)_6]\cdot nH_2O$ is synthesized and structurally characterized. A simple aqueous synthetic procedure for preparing nanoparticles of this novel coordination polymer is reported. The stability, in vitro ion exchange with ferrous ions, cytotoxicity, and cellular uptake of such nanoparticles coated with poly(vinylpyrrolidone) are investigated for potential applications of delivering Ga^{3+} ions into cells or removing iron from cells.

Metal hexacyanometallates $A_xM_y[M'(CN)_6]_z$ (A = alkali metal ions, M = main-group-, transition-, or lanthanide-metal ions, and M′ = Cr, Mn, Fe, or Co), constitute an important class of inorganic coordination polymers that have recently attracted increasing research attention.[1−4] PB can be prepared in two different forms, i.e., the soluble PB (SPB) with the idealized formula $KFe^{III}[Fe^{II}(CN)_6]$ and the insoluble PB (IPB) with the idealized formula $Fe_4^{III}[Fe^{II}(CN)_6]_3$. In recent years, transition- and lanthanide-metal analogues of PB have been intensively investigated for their magnetic and photomagnetic properties.[5−8] However, PB analogues of main-group metals have only previously been studied to a lesser extent.[1−3] Recently, there have been growing interests in the synthesis and investigations of novel nanoparticles derived from PB and its analogues.[9−12] Particularly scarce is the exploration of the coordination chemistry of the main-group-metal hexacyanometallates that have potential biomedical relevance.[13−17]

In living systems, gallium(III) may be viewed as a redox-inactive mimic of iron(III), as manifested by their similar biological transport and binding properties because of the identical charge and similar ionic radii of the two ions.[18−22] Recently, Singh et al. showed that certain gallium(III) compounds exhibit antimicrobial activities against the multidrug-resistant strains of *Pseudomonas aeruginosa* isolated from patients with cystic fibrosis by disrupting the bacterial uptake and metabolism of iron.[23] On the other hand, both Ga-67 (γ emitter with $t_{1/2}$ = 78.3 h) and Ga-68 (positron emitter with $t_{1/2}$ = 68 months) are delivered as the citrate complex in diagnostic nuclear medicine for γ-radiation or positron-emission imaging, respectively.[24,25] However, because of rapid decomplexation and hydrolysis, the mechanism of the uptake and biodistribution of these two radioisotopes in vivo is complicated and less desirable.[26,27] In general, the lack of stability and the complex hydrolysis of gallium compounds at physiological pH have hampered the further development of radioactive and nonradioactive gallium pharmaceuticals.[28,29]

In light of the resurgence of interest in the medicinal and radiopharmaceutical chemistry of gallium, here we describe the synthesis and characterization of the gallium analogue of SPB. Thus far, the gallium analogue of SPB has not been reported in the literature, while the preparation of thin films consisting of the gallium analogue of ISB has been described before.[30,31]

Upon mixing of the aqueous $Ga(NO_3)_3$ and $K_4[Fe(CN)_6]$ solutions with a molar ratio of 1:1 at concentrations of up to 0.25 M, neither an immediate color change nor a precipitate resulted. However, the solution did quickly turn turbid after mixing and registered a pH value of 5.3. Continuous stirring of the resultant solution at room temperature for more than 24 h afforded a slight color change to off-green, but no precipitation occurred. During the time of continual stirring, the solution showed a decreasing degree of turbidity. Additionally, even when an approximately equal volume of acetone was added to the above aqueous solution, the reaction product still did not separate from the liquid as a precipitate. Only after centrifugation at 13000 rpm for ca. 10 min did a pale-yellow pellet form at the bottom of the Eppendorf tube. The isolated precipitate could be redispersed back into water to form an almost colorless solution. This allowed for purification of the product through a water−acetone resuspension followed by centrifugation. Elemental analysis of the purified bulk materials by the atomic adsorption (AA) spectrometry gave a Ga−Fe ratio of 0.85:1.00 or an empirical formula $KGa_{0.92}Fe_{0.08}[Fe(CN)_6]$. These observations strongly suggest that the target compound has a strong tendency to form peptized colloidal particles reminiscent of the SBP system (vide infra).

The crystal structure of this new compound was determined by powder X-ray diffraction (XRD) on the bulk sample and found to be isostructural to the well-known SPR reported by Ludi et al. using the single-crystal structure analysis.[32] The Rietveld refinement was performed using *TOPAS* academic software (Figure S1 in the Supporting Information, SI).[33] Atomic positions were set to be the same as those of a similar SPB compound, $KNi[Fe(CN)_6]_{0.3}[Co(CN)_6]_{0.7}$, from the work by Widmann et al.[34] The final refinement in space group $Fm\bar{3}m$ yielded a = 10.1274(3) Å and V = 1038.7(1) Å^3 (see the SI for

Received: October 16, 2012
Published: March 6, 2013

   dx.doi.org/10.1021/ic302262g | *Inorg. Chem.* 2013, 52, 2790−2792

details of the structure refinement). The structure can be best viewed as the face-centered-cubic lattice defined by one type of ion, i.e., the Fe^{2+} or Ga^{3+} ions, with another type of ion, i.e., the Ga^{3+} or Fe^{2+} ions occupying the octahedral holes. The infinite 3D framework coordination polymer is then completed by CN^- groups (Figure 1).

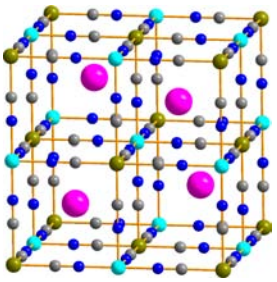

Figure 1. Unit cell structure of $KGa[Fe(CN)_6]$. Color code: dark yellow, Fe^{II}; turquoise, Ga^{III}; pink, K; gray, C; blue, N.

The Fourier transform infrared (FT-IR) spectra of the bulk sample exhibited a strong and broad C≡N stretching vibration centered at 2111 cm^{-1}, attributable to the Fe^{II}–C≡N–Ga^{III} bonding mode in the structure (Figure S2 in the SI). Next to this peak, a shoulder appeared at 2075 cm^{-1}. The latter is the characteristic stretching vibration attributed to the Fe^{II}–C≡N–Fe^{III} bonding mode found in pure PB samples.[35] This observation indicates the formation of a trace amount of PB as a contaminant due to the slow dissociation of $[Fe(CN)_6]^{4-}$ under acidic conditions during the synthesis and oxidation of the dissociated Fe^{2+} to Fe^{3+} by air.

Results from thermal gravimetric analysis (TGA) on the bulk sample showed a clean one-step 17.3% weight loss of water before heating to 150 °C, indicating the presence of ∼3.7 zeolitic water molecules per formula (Figure S3 in the SI). Similar to that found in SPB, the number of zeolitic water molecules varies from 3.7 to 4.0 from one batch to another of samples.

To better control the size distribution of and to impart biocompatibility to GaPBNPs, poly(vinylpyrrolidone) (PVP) was used as a surface coating agent.[36,37] PVP is a water-soluble and biocompatible polymer widely used in pharmaceuticals and cosmetics.[38,39] In a typical synthesis of PVP-coated GaPBNPs, an aqueous $Ga(NO_3)_3$ solution (1 mM, 50 mL) containing 200 mg of PVP (average MW = 8000) was slowly added to an aqueous $K_4[Fe(CN)_6]$ solution (1 mM, 50 mL) under vigorous stirring for 4 h, resulting in a slight color change to pale yellow. The product was isolated by centrifugation and purified by repeated resuspension of the product in water followed by centrifugation (see the SI). Transmission electronic microscopy (TEM) images of the PVP-coated nanoparticles revealed quasi-spherical nanoparticles with a narrow distribution of size at ca. 15 ± 2 nm (Figure 2), which was obtained from counting and averaging the size of 160 particles (Figure S4 in the SI). Additionally, distinctive signals of K, Ga, and Fe were detected by energy-dispersive X-ray spectroscopy performed on the same TEM sample (Figure S5 in the SI). Furthermore, the powder XRD pattern, FT-IR spectra, and TGA all confirmed that the inorganic core of the PVP-coated GaPBNPs is composed of the single-phased $KGa[Fe(CN)_6]$ (Figures S6–S8 in the SI). On the basis of the assumed Gaussian-type peak broadening, the average particle size can be estimated to be 10 ± 2 nm using the Scherrer formula.

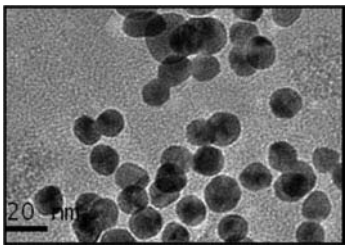

Figure 2. TEM image of PVP-coated GaPBNPs.

The stability of PVP-coated GaPBNPs dispersed in aqueous solution was monitored over a period of 4 weeks by dynamic light scattering. No change in the particle size and size distribution was detected during this time period (Figure S9 in the SI). We also monitored the leaching of Ga^{3+} ions due to dissociation and hydrolysis from PVP-coated nanoparticles to the solution and found that the gallium concentrations were below the detection level of 20 ppm by AA. The release of free cyanide ions from nanoparticles into the solution was studied by the Konig reaction.[40] The highest cyanide concentration detected after 24 h of incubation with GaPBNPs was below ∼0.15 ± 0.05 ppm at neutral pH.[41,42]

The in vitro ion exchange of GaPBNPs with ferrous ions was studied in air at neutral pH. The results showed that the ion-exchange reaction followed a pseudo-first-order reaction up to a reaction time of ∼50 min with a rate constant of $k_1 = 1.2 \times 10^{-2}$ min^{-1} or a half-life of $t_{1/2} = 58$ min (Figure S10 in the SI). There is an abrupt change of the reaction rate after this point to a slower and second-order reaction with a rate constant of $k_2 = 0.60$ M^{-1} min^{-1} (Figure S11 in the SI), presumably because of the need for Fe^{2+} ions to penetrate the GaPBNPs to react with the inner Ga^{3+} ions after the surface Ga^{3+} ions are consumed. It should be noted that the Fe^{2+} ions are oxidized by O atoms from air to become Fe^{3+} ions during ion exchange.

The cytotoxicity of GaPBNPs was evaluated using a trypan blue exclusion viability assay. After 24 h of incubation with a concentration of 1.1 mM, the cell viability was found to be ca. 95 ± 4% (Figure S12 in SI), suggesting that cell killing by the PVP-coated GaPBNPs does not occur for these types of cells under the experimental conditions.

The cellular uptake of PVP-coated GaPBNPs in HeLa cells was visualized using the confocal fluorescence microscopy technique. Nanoparticles were first conjugated with fluorescence dye molecules by a water-soluble carbodiimide coupling reaction (see the SI). The fluorescent images of the live HeLa cells treated with dye-labeled nanoparticles showed strong fluorescent signals in the perinuclear region of the cell, indicating an untargeted distribution of nanoparticles in the cytoplasm without specific binding to any of the small organelles in the region (Figure 3). This observation seems to suggest that the cellular uptake of these nanoparticles is via endocytosis.

In summary, we have synthesized and structurally characterized a novel potassium–gallium hexacyanoferrate(II), $KGa[Fe(CN)_6]\cdot nH_2O$. We have also developed a proper method for stabilizing the nanoparticles of this compound and have demonstrated their ion-exchange properties for removing iron from the aqueous solution. We have studied the biocompatibility of PVP-coated GaPBNPs using HeLa cells. Subsequently, we have shown that such nanoparticles can penetrate the cell membrane and hence are suitable for cellular and molecular imaging applications using gallium radioisotopes. Particularly

dx.doi.org/10.1021/ic302262g | Inorg. Chem. 2013, 52, 2790–2792

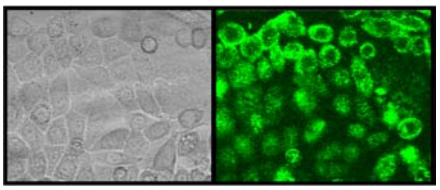

Figure 3. Bright-field (left) and confocal-fluorescence (right) images of dye-labeled GaPBNP-treated HeLa cells.

relevant to the development of novel gallium radiopharmaceuticals using this nanoplatform is its ability to form highly water-dispersible, but yet hydrolytically stable, nanoparticles at physiological pH. In addition, GaPB nanoparticles can sequester Fe^{2+} ions and release Ga^{3+} ions via a rapid ion-exchange reaction, suggesting possible antimicrobial activities of these nanoparticles.

■ ASSOCIATED CONTENT

Supporting Information

Figures S10−12, X-ray crystallographic data in CIF format and experimental details including synthesis, characterization, ion-exchange kinetics, cell viability, and uptake studies of PVP-coated GaPBNPs. This material is available free of charge via the Internet at http://pubs.acs.org.

■ AUTHOR INFORMATION

Corresponding Author

*E-mail: woodward@chemistry.ohio-state.edu (P.M.W.), shuang1@kent.edu (S.D.H.).

Notes

The authors declare no competing financial interest.

■ ACKNOWLEDGMENTS

We thank NIH-NCI for financial support (Grant 1R21CA143408-01A1) and NSF-CRIF for Grant CHE-1048645 to update the departmental NMR facility. The TEM data were obtained using the Cryo-TEM Facility at Liquid Crystal Institute, Kent State University, supported by the Ohio Research Scholars Program.

■ REFERENCES

(1) Dunbar, K. R.; Heintz, R. A. *Prog. Inorg. Chem.* **1997**, *45*, 283−391.
(2) Ludi, A.; Güdel, H. U. *Struct. Bonding (Berlin)* **1973**, *14*, 1−22.
(3) Robin, M. B.; Day, P. *Adv. Inorg. Chem. Radiochem.* **1967**, *10*, 247−422.
(4) Woodward, J. *Philos. Trans.* **1724**, *33*, 15−17.
(5) Ferlay, S.; Mallah, T.; Ouahès, R.; Veillet, P.; Verdaguer, M. *Nature* **1995**, *378*, 701−703.
(6) Entley, W. R.; Girolami, G. S. *Science* **1995**, *268*, 397−400.
(7) Sato, O.; Iyoda, T.; Fujishima, A.; Hashimoto, K. *Science* **1996**, *272*, 704−705.
(8) Holmes, S. M.; Girolami, G. S. *J. Am. Chem. Soc.* **1999**, *121*, 5593−5594.
(9) Vaucher, S.; Li, M.; Mann, S. *Angew. Chem., Int. Ed.* **2000**, *39*, 1793−1796.
(10) Moore, J. G.; Lochner, E. J.; Ramsey, C.; Dalal, N. S.; Stiegman, A. E. *Angew. Chem., Int. Ed.* **2003**, *42*, 2741−2743.
(11) Catala, L.; Volatron, F.; Brinzei, D.; Mallah, T. *Inorg. Chem.* **2009**, *48*, 3360−3370.
(12) Volatron, F.; Heurtaux, D.; Catala, L.; Mathoniere, C.; Gloter, A.; Stephan, O.; Repetto, D.; Clemente-Leon, M.; Coronado, E.; Mallah, T. *Chem. Commun.* **2011**, *47*, 1985−1987.
(13) Shokouhimehr, M.; Soehnlen, E. S.; Khitrin, A.; Basu, S.; Huang, S. D. *Inorg. Chem. Commun.* **2010**, *13*, 58−61.
(14) Shokouhimehr, M.; Soehnlen, E. S.; Hao, J.; Griswold, M.; Flask, C.; Fan, X.; Basilion, J. P. S.; Basu, S.; Huang, S. D. *J. Mater. Chem.* **2010**, *20*, 5251−5259.
(15) Chelebaeva, E.; Larionova, J.; Guari, Y.; Ferreira, R. A. S.; Carlos, L. D.; Trifonov, A. A.; Kalaivani, T.; Lascialfari, A.; Guerin, C.; Molvinger, K.; Datas, L.; Maynadier, M.; Gary-Bobo, M.; Garcia, M. *Nanoscale* **2011**, *3*, 1200−1210.
(16) Fu, G.; Liu, W.; Feng, S.; Yue, X. *Chem. Commun.* **2012**, *48*, 11567−11569.
(17) Lian, H.-Y.; Hu, M.; Liu, C.-H.; Yamauchi, Y.; Wu, K. C. W. *Chem. Commun.* **2012**, *48*, 5151−5153.
(18) Urena, E.; Garcia de Torres, A.; Cano Pavon, J. M.; Gomez Ariza, J. L. *Anal. Chem.* **1985**, *57*, 2309−2311.
(19) Llinas, M.; Wilson, D. M.; Neilands, J. B. *Biochemistry* **1973**, *112*, 3836−3843.
(20) Moerlein, S. M.; Welch, M. J.; Raymond, K. N. *J. Nucl. Med.* **1982**, *23*, 501−506.
(21) Nelson, W. O.; Karpishin, T. B.; Rettig, S. J.; Orvig, C. *Inorg. Chem.* **1988**, *27*, 1045−1051.
(22) Bandoli, G.; Dolmella, A.; Tisato, F.; Porchia, M.; Refosco, F. *Coord. Chem. Rev.* **2009**, *253*, 56−77.
(23) Kaneko, Y.; Thoendel, M.; Olakanmi, O.; Britigan, B. E.; Singh, P. K. *J. Clin. Invest.* **2007**, *117*, 877−888.
(24) Edwards, C. L.; Hayes, R. L. *J. Nucl. Med.* **1969**, *10*, 103−105.
(25) Bartholoma, M. D.; Louie, A. S.; Valliant, J. F.; Zubieta, J. *Chem. Rev.* **2010**, *110*, 2903−2920 and references cited therein.
(26) Bernstein, L. R.; Tanner, T.; Godfrey, C.; Noll, B. *Metal-Based Drugs* **2000**, *7*, 33−47.
(27) Singh, A. N.; Liu, W.; Hao, G.; Kumar, A.; Gupta, A.; Oz, O. K.; Hsieh, J.-T.; Sun, X. *Bioconjugate Chem.* **2011**, *22*, 1650−1662 and references cited therein.
(28) Zhang, Z.; Rettig, S. J.; Orvig, C. *Inorg. Chem.* **1991**, *30*, 509−515.
(29) Clevette, D. J.; Lyster, D. M.; Nelson, W. O.; Rihela, T.; Webb, G. A.; Orvig, C. *Inorg. Chem.* **1990**, *29*, 667−672.
(30) Yu, H.; Sheng, Q. L.; Zheng, J. B. *Electrochim. Acta* **2007**, *52*, 4403−4410.
(31) Eftekhari, A. *J. Electrochem. Soc.* **2004**, *151*, E297−E301.
(32) Buser, H. J.; Schwarzenbach, D.; Petter, W.; Ludi, A. *Inorg. Chem.* **1977**, *16*, 2704−2710.
(33) *TOPAS Academic, General Profile and Structure Analysis Software for Powder Diffraction Data*; Bruker AXS: Karlsruhe, Germany, 2004.
(34) Widemann, A.; Kahlert, H.; Petrovic-Prelevic, I.; Wulff, H.; Yakhmi, J. V.; Bagkar, N.; Scholz, F. *Inorg. Chem.* **2002**, *41*, 5706−5715.
(35) Nakamoto, K. *Infrared and Raman Spectra of Inorganic and coordination Compounds Part B: Applications in Coordination, Organometallic and Bioinorganic Chemistry*, 5th ed.; John Wiley & Sons, Inc.: New York, 1997; p 60.
(36) Uemura, T.; Kitagawa, S. *J. Am. Chem. Soc.* **2003**, *125*, 7814−7815.
(37) Uemura, T.; Ohba, M.; Kitagawa, S. *Inorg. Chem.* **2004**, *43*, 7339−7345.
(38) D'Souza, A. J. M.; Schowen, R. L.; Topp, E. M. *J. Controlled Release* **2004**, *94*, 91−100.
(39) Liu, X.; Sun, J.; Chen, X.; Wang, S.; Scott, H.; Zhang, X.; Zhang, Q. *J. Pharm. Pharmacol.* **2012**, *64*, 775−782.
(40) Yang, Y.; Brownell, C.; Sadrieh, N.; May, J.; Grosso, A. D.; Place, D.; Leutzinger, E.; Duffy, E.; He, R.; Houn, F.; Lyon, R.; Faustino, P. *Clin. Toxicol.* **2007**, *45*, 776−781.
(41) Vetter, J. *Toxicon* **2000**, *38*, 11−36.
(42) Cipollone, R.; Ascenzi, P.; Tomao, P.; Imperi, F.; Visca, P. *J. Mol. Microbiol. Biotechnol.* **2008**, *15*, 199−211.